Resonant soft-x-ray inelastic scattering from Gd in the $Gd_3Ga_5O_{12}$ garnet with excitation across the M_5 edge

C. Dallera,* L. Braicovich, and G. Ghiringhelli
Istituto Nazionale di Fisica della Materia and Dipartimento di Fisica, Politecnico di Milano, Piazza Leonardo da Vinci 32, I-20133, Milano, Italy

M. A. van Veenendaal, J. B. Goedkoop, and N. B. Brookes
European Synchrotron Radiation Facility, Boîte Postale 220, F-38043 Grenoble Cedex, France
(Received 24 October 1996)

We present resonant soft-x-ray scattering measurements across the M_5 edge of Gd in $Gd_3Ga_5O_{12}$. Below or near the Gd M_5 edge the scattering is dominated by the elastic contribution, whereas the inelastic contribution becomes dominant above the edge. The theoretical cross section is calculated in an ionic multiplet model, and the spectra are simulated by including self-absorption and saturation effects. The calculations account for all the measured features. It is shown that the inelastic contributions to the spectra are due to $4f$ spin-flip excitations, bringing Gd to a lower spin state in the final state. [S0163-1829(97)01620-2]

I. INTRODUCTION

In soft-x-ray spectroscopy a rapidly developing field is resonant x-ray scattering (RXRS), mainly due to the use of synchrotron radiation. Here we consider experiments in which a core hole is created by the incident photon via resonant excitation in the threshold region, and is then neutralized by a valence electron, with decay of the system to the ground state or to one of a manifold of excited states. The RXRS spectral function is thus *a priori* dependent on the incoming photon energy $h\nu_{\rm in}$ and the outgoing photon energy $h\nu_{\rm out}$. By measuring the outgoing photon energy in an experiment where several excitation energies are used, one has access to information that would be lost if an integration over the outgoing photon energy is made as, e.g., in fluorescence total yield measurements.

The recent possibility of carrying out RXRS experiments in the soft-x-ray range is of great help in the study of rare earths, a field where, to the author's knowledge, very limited information is available,[1,2] due to the difficulty of these experiments with low counting rate and very large self-absorption effects. In strongly correlated systems like rare earths a multiplet description of the electronic states is very often appropriate.[3] In this case multiplet splitting gives rise to significant structures in the RXRS spectra and to significant modifications of these features when $h\nu_{\rm in}$ is swept across an absorption edge. The present soft-x-ray experiment allows us to look at d-f transitions governed by the dipole operator. Previously, the quadrupolar contribution to Gd^{3+} RXRS has been observed in an experiment made on the same garnet with excitation at the L_3 absorption edge.[4] Resonant x-ray scattering from rare earths has been shown to be a powerful tool also in the resonant Raman regime,[5] where the created core hole is filled through an inner shell transition from an upper core level. Also in this case, any modification of the Raman spectrum when the excitation energy is scanned through the threshold is an indication of multiplet splitting effects.

The importance of multiplet splitting in rare-earth $M_{4,5}$ absorption is well known, and gives rise to spectral functions which can be simulated quite accurately with ionic model calculations.[3] In this connection RXRS experiments add information in spite of the above-mentioned difficulties (counting rate and self-absorption). In particular we show that in Gd^{3+} one can measure very small but important details of the spectral function, giving a direct insight in the excitation properties of the system. Gd^{3+} is an interesting model system due to the simplicity of the electronic structure, allowing a rather direct interpretation of the spectral function. We present results of a RXRS experiment at the Gd M_5 edge in the $Gd_3Ga_5O_{12}$ garnet. We measure the spectral function when a core hole is created close to threshold in the $3d_{5/2}$ level, and the $3d^9 4f^{n+1}$ excited state decays again into one of the $3d^{10}4f^n$ configuration multiplet terms, n being the ground state occupation number, i.e., 7 (the Hund rule high-spin state). In this way we show final states corresponding to $4f$ excitation with spin flip in agreement with the predictions of an ionic multiplet calculation. The garnets are very convenient, since they are very well-characterized systems. This particular garnet has the advantage that with our experimental setup it is possible to measure simultaneously the M_5 emission from Gd (around 1184 eV) and the L_3 and L_2 emission from Ga (around 1120 eV). This helps in the energy calibration and in the evaluation of the self-absorption corrections as will be shown below.

II. EXPERIMENT

The experiment was performed on ID12B at the European Synchrotron Radiation Facility in Grenoble. This beamline[6] covers the 500–1600-eV range, and uses a helical undulator.[7] The beamline monochromator is of the Dragon type.[8] The Gd M_5 RXRS spectra of a $Gd_3Ga_5O_{12}$ bulk sample were recorded with a grating spectrograph allowing parallel acquisition with constant resolution in a 40-eV energy interval. The energy window was centered on the Gd M_5 emission line, and the Ga lines were detected at lower

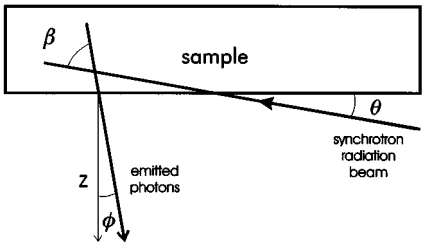

FIG. 1. Geometrical setup of the scattering experiment. The angle between the incoming beam and the sample surface is $\theta = 10°$, the scattering angle is $\beta = 110°$, the angle between the outgoing beam and the normal to the sample surface is $\phi = 10°$, and the coordinate along the normal is z.

resolution (this still allowed to use their energy position for energy calibration, and their integrated intensity for intensity cross-check). This instrument has been extensively described elsewhere.[9] The spectrograph is matched to the exit slit of the beamline monochromator with a Kirkpatrick-Baez refocusing optics. In order to increase the counting rate we chose a 2.5-eV bandpass in the excitation channel, and a 3-eV bandpass in the analyzer. The typical integrated counting rate on the whole Gd peak was 1–1.5 counts/s, with 160 mA in the ring. The sample was a single-crystal platelet having a well-defined surface. The angle between the sample surface and the incident beam was 10° to reduce self-absorption. The angle between the k vector of the scattered radiation and the k vector of the incident photons was 110° in the horizontal plane. The geometrical setup of the experiment is shown in Fig. 1.

The x-ray-absorption spectrum was obtained in the same apparatus from the sample drain current. The measurement was optimized by facing a high-voltage electrode to the sample (field around 2 kV/cm) to extract the drain current, avoiding charging. In this case the bandpass in the excitation channel was there set to 0.8 eV.

When measuring the scattering spectra excited below or above threshold, after every 2-h acquisition a reference spectrum was taken with the excitation energy set to the main absorption peak ($h\nu = 1184.5$ eV), in order to check the stability.

III. RESULTS AND DISCUSSION

A. Experimental results: A qualitative discussion

An overview of the RXRS results are given in Fig. 1 (lower panel), where we present the scattering spectral functions normalized to the acquisition time and to the current in the ring for the excitation energies given by the arrows along the M_5 absorption spectrum (Fig. 2, upper panel). The spectra include the resonant Gd contribution and the Ga $L_{2,3}$ fluorescence due to the photons absorbed by Ga $2p$ well above threshold (i.e., in a nonresonant mode). Some important trends concerning the shape of the Gd spectra and the intensity of the Ga and Gd lines are immediately evident from Fig. 2.

Shape of the spectra. The Gd spectra excited below and at threshold (cases 1 and 2) are dominated by an elastic peak found at the energy of the excitation channel within the accuracy allowed by the bandwidth. The position of the elastic

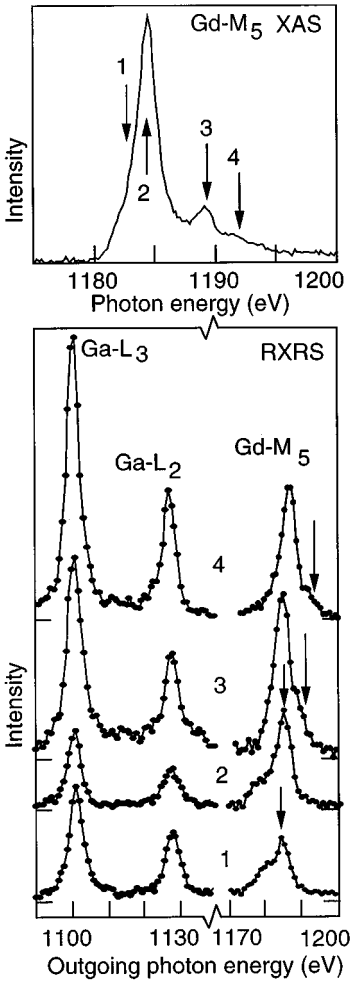

FIG. 2. Measured scattering spectra (lower panel) from $Gd_3Ga_5O_{12}$ excited at different photon energies indicated by the arrows along the Gd M_5 absorption spectrum (upper panel). The Gd M_5 and Ga $L_{2,3}$ lines have been recorded simultaneously. The vertical arrows in the lower panel give the position of the elastic scattering contribution.

contribution is marked by the arrows in Fig. 2. It is apparent that the elastic contribution is still present with excitation above threshold (cases 3 and 4), where it becomes a small fraction of the total intensity. In all the spectra an inelastic contribution is seen at energies lower than that of the elastic peak, and corresponding to an excited final state obtained from the decay of the intermediate $3d^9 4f^8$ configuration into one of the $3d^{10}4f^7$ final states. The first excited states are obviously above the Hund-rule ground state, so that we expect that the inelastic contribution is due to a $4f$ spin flip. This important point will be considered in more detail below in the comparison with theory. This will also explain the evolution of the intensities from cases 1 and 2, dominated by the elastic scattering, to cases 3 and 4, dominated by the inelastic scattering.

Integrated intensities. The intensities of the Ga lines depend on the excitation energy in spite of the fact that the Ga $2p$ excitation cross section is basically constant in our excitation range.[10] This is due to the removal of photons caused by the strong absorption of the Gd $3d_{5/2}$ level. By using the

absorption coefficients to the continuum for Ga and O and for Gd below threshold from the literature,[8] one can calculate the Gd absorption which is expected on the basis of the measured evolution of the Ga intensities. The calculation is simple and reliable since the self-absorption of the $L_{2,3}$ Ga fluorescence photons is negligible. The calculated Gd absorption coefficients follow our absorption measurements (drain current) within 10%. This is a very important consistency test of our absorption coefficients and intensities. In this test we have made the implicit assumption that the integrated intensity of the lines emitted by Ga reproduces the Ga absorption coefficient. This is a good assumption, since Ga is excited far from resonance, and therefore the branching ratio between radiative and nonradiative decay does not depend on the excitation energy in our energy range.

It is also possible to extract further information from the Gd intensities which have a nontrivial dependence on the excitation energy. In fact the scattered intensity from Gd is smaller with excitation at the edge (where the absorption coefficient has its largest value) than with excitation below the edge. This is largely due to saturation and self-absorption effects that modify significantly the measured spectra. At a more fundamental level another possible origin is the excitation energy dependence of the branching ratio between radiative and nonradiative Auger decay, preventing the use of total fluorescence to measure the absorption.[11] We evaluated the saturation and self-absorption effects by calculating (on the basis of the Gd absorption drain current) the total Gd intensity one would expect with a constant branching ratio to the Auger. The results are affected by the innaccuracy of the parameters, but there is no doubt that self-absorption and saturation are very important since Gd excited at threshold emits a very strong elastic peak whose intensity ratio to background is about 100. However, this does not explain the whole deviation of the integrated Gd spectra from the absorption spectrum. The remaining discrepancy can be explained by assuming that the branching ratio is energy dependent and increases. According to our evaluation it increases by a factor of 2 ± 0.2 on passing from $h\nu_{\rm in}=1184.5$ eV to $h\nu_{\rm in}=1191.9$ eV. The discussion of this point is beyond the purpose of the present work, but could be an interesting subject of future research also requiring complementary resonant Auger measurements. In what follows we greatly simplify the problem by disregarding the energy dependence of this branching ratio. However, a nonnegligible result of the present work is to show that all main features of the measured spectra can still be understood in this simplified scheme.

B. Theoretical results

Here we present the theoretical atomic cross sections for the radiative channel calculated without including the effects of the bandpass, and saturation and self-absorption effects. This is a rather ideal case which is very illuminating in the discussion of the experiment.

Spectra were calculated using Cowan's program.[12] The x-ray inelastic cross section is

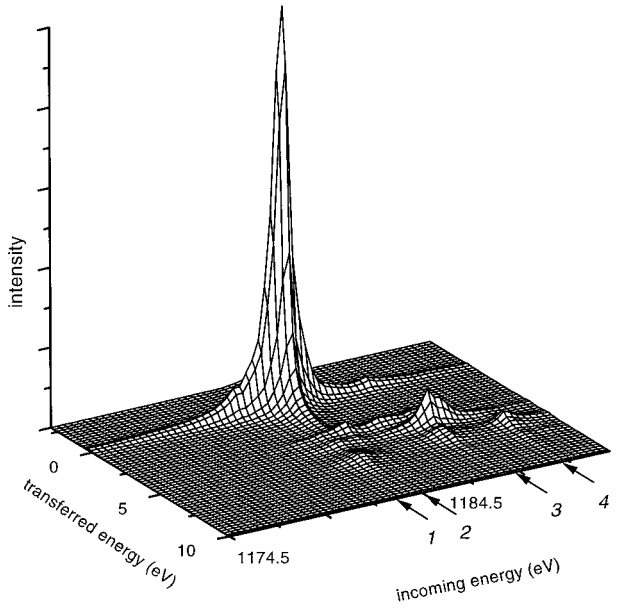

FIG. 3. Calculated Gd M_5 scattering cross section plotted as a function of the ingoing energy $h\nu_{\rm in}$ and of the transferred energy $T=(h\nu_{\rm in}-h\nu_{\rm out})$. The arrows along the $h\nu_{\rm in}$ scale indicate the excitation energies used in the present experiment.

$$I(\nu_{\rm in},\nu_{\rm out})=\frac{\Gamma}{\pi}\frac{\nu_{\rm out}}{\nu_{\rm in}}\sum_f\left|\sum_n\frac{\langle f|D^{(1)}|n\rangle\langle n|D^{(1)}|g\rangle}{E_g+h\nu_{\rm in}-E_n+i\,\frac{\Gamma}{2}}\right|^2\times\delta(E_g+h\nu_{\rm in}-E_f-h\nu_{\rm out}). \quad (1)$$

Parameters were obtained within the Hartree-Fock limit, and scaled down to 80% to account for intra-atomic screening effects. For a Gd^{3+} ion the configurations starting from the $|g\rangle=|4f^7;{}^8S_{7/2}\rangle$ ground state are $|n\rangle=|3d^94f^8\rangle$, and $|f\rangle=|4f^7\rangle$ for the intermediate and final states, respectively. The total $3d^94f^{n+1}$ multiplet structure is extremely complex, and thousands of levels are present for rare earths in the middle of the series. The number of states which can be reached from the ground-state configuration is greatly reduced by dipole selection rules $\Delta J=0,+1,-1$, but is still very large. After inclusion of the lifetime effects (about 1-eV Lorentzian broadening[13]) a simple shape is obtained which nevertheless carries a lot of important information, as already shown in the simpler problem of core-level absorption.[3]

Figure 3 shows the results of the calculation in the M_5 region as a function of the ingoing energy $h\nu_{\rm in}$ and of the transferred energy $T=(h\nu_{\rm in}-h\nu_{\rm out})$ which are the natural coordinates in the calculation of the cross section with formula (1). In an ideal experiment with infinite resolution and without saturation and self-absorption effects, a measured spectrum has the shape of a section of Fig. 3 with a vertical plane parallel to the transferred energy axis (the energies used in the present experiment are given by the arrows). The theoretical results of Fig. 3 clearly show the following features:

(i) The elastic peak (transferred energy $T=0$) is the dominant contribution with excitation at threshold and below threshold (within the lifetime broadening).

(ii) The main inelastic region corresponding to about 5-eV transferred energy is dominant for excitation well above threshold (cases 3 and 4). This corresponds to the spin flip, so that the final state has lower spin. Although the dipole operator conserves spin it is still possible to make a transition from the octet ground state to a sextet final state since in the intermediate state spin is not a good quantum number. The spin-flip transitions mainly occur on the high-energy side of the edge. We can understand this as follows. Within LS coupling the average energy of the $3d^9 4f^8$ intermediate state with $S=\frac{7}{2}$ is lower than of those with $S=\frac{5}{2}$. Therefore the large $3d$ spin-orbit coupling mixes the $S=\frac{7}{2}$ states more strongly with low-spin states at the high-energy side of the edge compared to the low-energy side.

(iii) Both the elastic and inelastic features have tails extending along the incoming energy axes, so that both features should be seen in the spectra with a dominant elastic contribution at low excitation energies (cases 1 and 2) and dominant inelastic contribution at higher excitation energies (cases 3 and 4). Note that the resonant excitation of one of the two dominating regions (elastic or inelastic) also slightly reinforces the tail of the other contribution due to coupling effects included in formula (1).

This theoretical behavior is in good qualitative agreement with the experimental trend presented above. Thus the basic physics of the atomic cross section is directly accessible even without simulating the experiment in detail.

C. Comparison between theory and experiment

As discussed above, a detailed comparison with the experiment implies a simulation including saturation and self-absorption effects. Before accounting for the bandpass, this has been done by integrating the following formula:

$$I_{\mathrm{Gd}}(h\nu_{\mathrm{in}},h\nu_{\mathrm{out}}) \propto \int_0^{\infty} \sigma(h\nu_{\mathrm{in}},h\nu_{\mathrm{out}})[\exp(-z\alpha_{\mathrm{in}_{\mathrm{tot}}}/\sin\theta) \times \exp(-z\alpha_{\mathrm{out}_{\mathrm{tot}}}/\cos\phi)]dz, \quad (2)$$

where $I_{\mathrm{Gd}}(h\nu_{\mathrm{in}},h\nu_{\mathrm{out}})$ is the measured Gd spectrum, $\sigma(h\nu_{\mathrm{in}},h\nu_{\mathrm{out}})$ is the theoretical Gd scattering cross section, α_{intot} is the total absorption coefficient at the energy of the incoming photon, α_{outtot} is the total absorption coefficient at the energy of the outgoing photon, θ is the angle between the incoming beam and the sample surface, ϕ is the angle between the outgoing beam and the normal to the sample surface, and z is the coordinate normal to the surface (see Fig. 1). This formula assumes that the branching ratio with the Auger decay channel is constant. In the formula we have used the absorption coefficients taken from spectra measured in the transmission mode which perfectly agree with ours, and which provided us with absolute values.[14] After that we accounted for all bandpass effects. Note that, before doing this, each elementary calculated spectrum due to a single energy within the excitation bandpass has to be shifted properly, since the experimental spectra are measured as a function of $h\nu_{\mathrm{out}}$ while the theoretical spectra are calculated as a function of $T=(h\nu_{\mathrm{in}}-h\nu_{\mathrm{out}})$. The simulated spectra are given in Fig. 4 (solid heavy lines), where they are compared with the measurements after normalization to the same peak height. We are only interested in the shapes, since the intensities can be affected by the nonconstant branching ratio to the Auger decay channel. The spectra are plotted vs $h\nu_{\mathrm{out}}$, and this is very useful to understand how self-absorption affects the measurements. Each theoretical spectrum is decomposed into the elastic (thin solid line) and inelastic (dashed line) contributions. The vertical heavy dashed line gives the ideal elastic contribution whose energy increases linearly with $h\nu_{\mathrm{in}}$. In the simulation a small deviation with respect to this position is found only for the elastic line below threshold, since the bandpass includes contributions at different energies with very different weights due to the rapidly increasing absorption coefficient below threshold. This effect is also clearly seen in the measurements. In each measured spectrum the data points are plotted together with the theoretical shape of the dominant contribution (elastic in

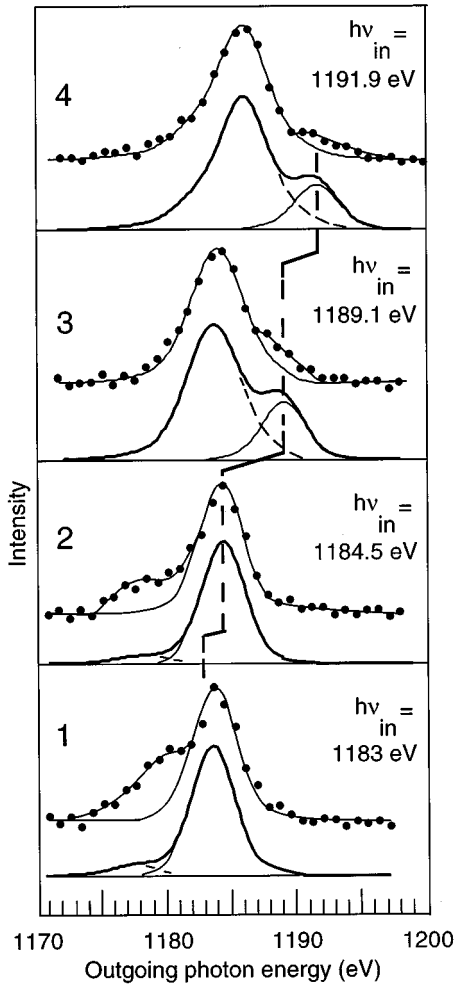

FIG. 4. Comparison between theory and experiment in resonant soft-x-ray scattering from $Gd_3Ga_5O_{12}$. The theoretical simulation, including saturation and self-absorption effects, is given by the heavy solid lines. The spectra are normalized to the same height to emphasize the modification of the shape. The inelastic and elastic contributions to the theoretical spectra are given by the dashed and thin solid lines, respectively. The heavy vertical dashed lines give the peak position of an elastic experiment with vanishing bandpass. The measurements are given by the dots. Each experimental spectrum is well fitted by the theoretical curve given by the dominant theoretical contribution to the spectra, i.e., the elastic peak in cases 1 and 2, and the inelastic peak in cases 3 and 4.

cases 1 and 2, and inelastic in cases 3 and 4). This gives an excellent fit of the spectra, and clearly puts into evidence the minority contributions where all data points are consistently above the fitting lines. This minority contribution is due to inelastic scattering in cases 1 and 2, and to elastic scattering in cases 3 and 4. We find an excellent agreement between theory and experiment as far as the dominant contribution to the spectra is concerned. Also, the separation between the elastic and inelastic features, which is the energy needed to flip a spin, is very consistent between theory and experiment. It should be noted that the inelastic peaks in cases 3 and 4 correspond to scattered photons having energies close to the very strong Gd absorption peak, so that a non-negligible line-shape distortion is generated with respect to the section with vertical planes at constant $h\nu_{\mathrm{in}}$ of the atomic cross sections given in Fig. 3. The measurements allow us to show also the small elastic contributions in cases 3 and 4, corresponding to less than 1% of the peak value of the atomic cross section, showing the sensitivity which can be reached with synchrotrons of the third generation. On the other hand the relative intensities of the dominant and minor contributions to the spectra are only in qualitative agreement with the theory. This point cannot be discussed in depth within the present scheme, due partly to the difficulties in making the self-absorption corrections but also because of the approximation of a constant branching ratio to the Auger process. However, the agreement between theory and experiment can be considered very satisfactory, so that the present data give for the first time, to our knowledge, direct and conclusive evidence of spin-flip excitations at the M threshold of rare earths with a good description of the spin-flip line shape. This result in the Gd case is analogous to the d-d excitations of the high-spin Mn d^5 configuration in MnO recently observed[15] with resonant inelastic soft-x-ray scattering.

IV. CONCLUSIONS

We have presented experimental results for resonant soft-x-ray scattering across the M_5 edge of Gd in $Gd_3Ga_5O_{12}$, showing a significant modification of the spectral functions when the excitation energy spans the $3d$-$4f$ resonance. Below and near the edge the scattering is dominated by the elastic contribution, whereas the inelastic contribution becomes dominant with excitation well above the edge. The inelastic contribution is due to the $4f$ spin-flip process, bringing Gd to a lower spin configuration in the final state, as shown clearly by a detailed comparison with multiplet calculations in an ionic model. A simulation including self-absorption and saturation and having a constant branching ratio between radiative and nonradiative decay accounts for all the measured features. Thus the method gives direct access to the energy scale characteristic of the $4f$ spin flip. To the authors' knowledge this is the first experimental evidence of this kind based on resonant M-edge x-ray scattering. This approach is potentially interesting in many situations in rare-earth spectroscopy.

ACKNOWLEDGMENTS

The authors wish to thank A. Rogalev for very helpful discussion during the experiment. Work was done under an AXES contract (European Synchrotron Radiation Facility and Istituto Nazionale Fisica Materia).

*Present address: European Synchrotron Radiation Facility, B.P. 220, F-38043 Grenoble Cedex, France.

[1] S. M. Butorin, D. C. Mancini, J.-H. Guo, N. Wassdahl, and J. Nordgren, J. Alloys Compd. **225**, 230 (1995).

[2] S. M. Butorin, D. C. Mancini, J.-H. Guo, N. Wassdahl, J. Nordgren, M. Nakazawa, S. Tanaka, T. Uozumi, A. Kotani, Y. Ma, K. E. Myano, B. A. Karlin, and D. K. Shuh, Phys. Rev. Lett. **77**, 574 (1996); **77**, 574 (1996).

[3] B. T. Thole, G. van der Laan, and J. C. Fuggle, G. A. Sawatzky, R. C. Karnatak, and J.-M. Esteva, Phys. Rev. B **32**, 8 (1985); **32**, 5107 (1985).

[4] M. H. Krisch, C. C. Kao, F. Sette, W. A. Caliebe, K. Hämäläinen, and J. B. Hastings, Phys. Rev. Lett. **74**, 4931 (1995).

[5] P. Carra, M. Fabrizio, and B. T. Thole, Phys. Rev. Lett. **74**, 3700 (1995).

[6] J. Goulon, N. B. Brookes, C. Gauthier, J. B. Goedkoop, C. Goulon-Ginet, M. Hagelstein, and A. Rogalev, Physica B **208&209**, 199 (1995).

[7] P. Elleaume, J. Synchrotron. Radiat. **1**, 19 (1994), and references therein. The undulator produces circularly polarized radiation that is immaterial to the purpose of this work: in fact $Gd_3Ga_5O_{12}$ does not have a magnetically ordered structure. Therefore there is no preferential quantization axis, which means that an integration over all different polarization directions takes place, and that the light can be considered isotropic.

[8] C. T. Chen, Nucl. Instrum. Methods Phys. Res. A **256**, 595 (1987).

[9] C. Dallera, E. Puppin, G. Trezzi, N. Incorvaia, A. Fasana, L. Braicovich, N. B. Brookes, and J. B. Goedkoop, J. Synchrotron. Radiat. **3**, 231 (1996).

[10] B. L. Henke, P. Lee, T. J. Tanaka, R. I. Shimabukuro, and B. K. Fujikawa, At. Data Nucl. Data Tables **27**, 1 (1982).

[11] F. M. F. de Groot, M. A. Arrio, Ph. Sainctavit, Ch. Cartier, and C. T. Chen, Solid State Commun. **92**, 991 (1994).

[12] R. D. Cowan, *The Theory of Atomic Structure and Spectra* (University of California Press, Berkeley, 1981).

[13] O. Keski-Rahkonen and M. O. Krause, At. Data Nucl. Data Table **14**, 139 (1974).

[14] F. C. Vicentin, S. Turchini, F. Yubero, J. Vogel, and M. Sacchi, J. Electron Spectrosc. Relat. Phenom. **74**, 187 (1995).

[15] S. M. Butorin, J.-H. Guo, M. Magnuson, P. Kuiper, and J. Nordgren, Phys. Rev. B **54**, 4405 (1996).